Neurobiology of Disease

Mutations in the Microtubule-Associated Protein 1A (*Map1a*) Gene Cause Purkinje Cell Degeneration

Ye Liu, Jeong Woong Lee, and Susan L. Ackerman
Howard Hughes Medical Institute, The Jackson Laboratory, Bar Harbor, Maine 04609

The structural microtubule-associated proteins (MAPs) are critical for the organization of neuronal microtubules (MTs). Microtubule-associated protein 1A (MAP1A) is one of the most abundantly expressed MAPs in the mammalian brain. However, its *in vivo* function remains largely unknown. Here we describe a spontaneous mouse mutation, *nm2719*, which causes tremors, ataxia, and loss of cerebellar Purkinje neurons in aged homozygous mice. The *nm2719* mutation disrupts the *Map1a* gene. We show that targeted deletion of mouse *Map1a* gene leads to similar neurodegenerative defects. Before neuron death, *Map1a* mutant Purkinje cells exhibited abnormal focal swellings of dendritic shafts and disruptions in axon initial segment (AIS) morphology. Furthermore, the MT network was reduced in the somatodendritic and AIS compartments, and both the heavy and light chains of MAP1B, another brain-enriched MAP, was aberrantly distributed in the soma and dendrites of mutant Purkinje cells. MAP1A has been reported to bind to the membrane-associated guanylate kinase (MAGUK) scaffolding proteins, as well as to MTs. Indeed, PSD-93, the MAGUK specifically enriched in Purkinje cells, was reduced in *Map1a*$^{-/-}$ Purkinje cells. These results demonstrate that MAP1A functions to maintain both the neuronal MT network and the level of PSD-93 in neurons of the mammalian brain.

Key words: **cerebellum; Dlg2; MAP1A; microtubule; neurodegeneration; Purkinje cell**

Introduction

Microtubules (MTs) are essential for the specification and maintenance of polarized cellular structures and intracellular transport in neurons. The stability of the MT lattice is largely regulated by the binding of the structural subgroup of the microtubule-associated proteins (MAPs), including tau, MAP2, MAP1A, and MAP1B (Conde and Cáceres, 2009). Like MTs, which are distinctly organized in dendrites and axons, the structural MAPs display characteristic subcellular localization patterns in neurons. Tau is enriched in axons, whereas MAP2 is mainly localized to the somatodendritic domain of neurons. The two members of the MAP1 family, MAP1A and MAP1B, are also discretely localized (Halpain and Dehmelt, 2006). MAP1A is primarily localized to the somatodendritic compartment in the adult brain, although it is also present in a subset of axons (Huber and Matus, 1984b; Schoenfeld et al., 1989; Szebenyi et al., 2005). By contrast, MAP1B is enriched in growing axons during early brain development (Schoenfeld et al., 1989).

Mutation studies have illustrated the importance of the structural MAPs in the mammalian brain. Mutations in tau cause autosomal-dominant frontotemporal dementia and parkinsonism linked to chromosome 17 (FTDP-17) in human (Goedert and Jakes, 2005). Furthermore, abnormal formation of fibrillar tau inclusions is a hallmark of many human neurodegenerative diseases, known as tauopathies (Ballatore et al., 2007). Additionally, *tau* knock-out mice display age-dependent neurodegeneration and cognitive deficits (Lei et al., 2012). In contrast to *tau* mutations, loss of *Map2* or *Map1b* causes neurodevelopmental abnormalities. Dendritic length and dendritic MT density are reduced in *Map2*$^{-/-}$ neurons (Harada et al., 2002) and MAP1B deletion results in axonal guidance defects (Meixner et al., 2000; Bouquet et al., 2004).

For most structural MAPs, the *in vivo* consequences of deficiencies have been reported, but this is not the case for MAP1A. The *Map1a* gene encodes a precursor polypeptide that is proteolytically cleaved to produce a MAP1A heavy chain (MAP1A-HC) and a light chain (LC2; Langkopf et al., 1992). These proteins can bind to MTs independently or as a complex that can include LC1, a proteolytic cleavage product from MAP1B precursor protein (Hammarback et al., 1991), and LC3, an independently encoded autophagosomal protein (Vallee and Davis, 1983; Mann and Hammarback, 1994; Kabeya et al., 2000). In addition to binding with MT, MAP1A-HC interacts with the membrane-associated guanylate kinases (MAGUKs) through a C-terminal consensus domain (Brenman et al., 1998; Reese et al., 2007).

Here we report that MAP1A mutation causes ataxia, tremors, and late-onset degeneration of cerebellar Purkinje cells, which

Received July 7, 2014; revised Jan. 19, 2015; accepted Jan. 23, 2015.

Author contributions: Y.L. and S.L.A. designed research; Y.L. and J.W.L. performed research; Y.L., J.W.L., and S.L.A. analyzed data; Y.L. and S.L.A. wrote the paper.

Services used in this study were supported by Cancer Center Core Grant CA34196 (The Jackson Laboratory). We thank Lynne Beverly-Staggs for technical assistance. We also thank the Jackson Laboratory sequencing, histology, imaging, and microinjection services for their contributions; Dr. Michael Wiles and Peter Kutny for transgenic mouse production; Jennifer Torrance for video recording; Dr. Ken Johnson for helpful discussions on the project; and Dr. Mridu Kapur for comments on the manuscript. We thank Dr. Leah Rae Donahue and the Mouse Mutant Resource (supported by NIH OD10972), for identifying the *nm2719* mutant, and Coleen Kane, for doing the initial histology. S.L.A. is an investigator of the Howard Hughes Medical Institute.

The authors declare no competing financial interests.

Correspondence should be addressed to Dr. Susan L. Ackerman, The Jackson Laboratory, 600 Main Street, Bar Harbor, ME 04609. E-mail: susan.ackerman@jax.org.

J.W. Lee's present address: Korea Research Institute of Bioscience and Biotechnology (KRIBB), 125 Gwahak-ro, Yuseong-gu, Daejeon 305-806, Korea.

DOI:10.1523/JNEUROSCI.2757-14.2015

 0270-6474/15/354587-12$15.00/0

are preceded by structural abnormalities in Purkinje cell dendrites and the axon initial segment (AIS). We demonstrate that MT networks are altered in mutant Purkinje cells and that both the heavy and light chain of MAP1B is abnormally distributed in soma and dendrites of these neurons before structural defects. Furthermore, MAP1A deficiency results in decreased PSD-93 (also known as Chapsyn-110 or Dlg2) in Purkinje cells, suggesting that MAP1A is required to maintain normal levels of this MAGUK protein. Together, our results demonstrate the importance of MAP1A in neuronal MT organization, synaptic protein modulation, and neuronal survival in the adult CNS.

Materials and Methods

Mice. All animal protocols were approved by the Animal Care and Use Committee of The Jackson Laboratory. The *nm2719* mouse stain was maintained on the C57BLKS/J background. Tg-Map1a mice were a kind gift from Dr. Akihiro Ikeda at the University of Wisconsin-Madison, and this strain was maintained on the C57BL/6J background (Ikeda et al., 2002). For transgenic rescue experiments, Tg-Map1a mice were crossed with *nm2719*$^{-/-}$ mice for two generations to obtain Tg-Map1a; *nm2719*$^{-/-}$ offspring. The *Map1a* knock-out ES cells (C57BL/6NJ-*Map1a*$^{tm1(KOMP)Mbp}$) were obtained from the Knockout Mouse Project Repository (www.komp.org). Chimeras were bred to C57BL/6NJ mice, and heterozygous mice carrying the knock-out allele were bred to B6.129S4-*Gt(ROSA)26Sor*$^{tm1(FLP1)Dym}$/RainJ mice (Farley et al., 2000; the Jackson Laboratory) to remove the flippase recombinase target sites-flanked *lacZ*/*neo* cassettes (*Map1a*$^{tm1.2}$). To generate the neural-specific LC2 transgene construct, three Myc epitope tags were cloned in frame to the C terminus of the mouse *Map1a* genomic sequence encoding the light chain (2766–3014 aa), and this sequence was inserted downstream of the neuron-specific enolase (NSE) promoter (Twyman and Jones, 1997). This construct (pNSE-LC2–3Myc) was injected into the pronucleus of *nm2719*$^{+/-}$ embryos, and founder mice carrying the transgene were identified by PCR and mated to *nm2719*$^{-/-}$ mice.

The *nm2719* allele was differentiated from the wild-type (WT) allele by PCR using the Map1a-F (5′-GCTGAGTCGCCAGTTGGCTT-3′) and Map1a-R (5′AGTCATCTCAGGTGGGGATG-3′) primers; the *nm2719* amplicon is made up of 92 bp and WT amplicon is made up of 99 bp. Tg-Map1a transgenic mice were identified with the TgMap1a-F (5′-TC TGGGACCTCACTCCTCTG-3′) and TgMap1a-R (5′-TCTTGGTGAG TTCCCCTGAG-3′) PCR primers. The transgene, derived from 129P2/OlaHsd sequence, generated a 228 bp amplicon, while C57BLKS/J or C57BL/6J alleles generated a 150 bp amplicon due to a polymorphic microsatellite. To distinguish Tg-Map1a; *nm2719*$^{-/-}$ mice from Tg-Map1a; *nm2719*$^{+/-}$ mice, a WT allele-specific PCR primer Map1a-wtF (5′-GAGGAGGAGGACAAACTGAC-3′) was paired with TgMap1a-R. This primer pair amplified WT (both transgenic and endogenous) alleles, but not the *nm2719* allele, and the PCR products were sequenced to distinguish the transgenic versus the endogenous *Map1a* WT allele. The *Map1a*^{tm1} allele (with the *lacZ*/*neo* cassettes) was genotyped with the primer pair RAF5 (5′-CACACCTCCCCCTGAACCTGAAAC-3′) and Map1a-in5DR (5′-CCCACTTTCCTGATATACTCAC-3′). The *Map1a*$^{tm1.2}$ allele (lacking the *lacZ*/*neo* cassettes) was identified with Map1a-in5UF (5′-CCCCAATGATTTGATCAGCTTC-3′) and Map1a-in5DR primers. The Tg-pNSE-LC2–3Myc allele was genotyped with primer pair Map1a-lastXnF (5′-GTGACTCTGATTCCCACTCATG-3′) and 3T4AR (5′-GT GGTACACTTACCTGGTACC-3′). All PCR conditions were as follows: 35 cycles at 94°C for 30 s, 58°C for 30 s, and 72°C for 30 s. Both male and female mice were used in our studies and no sex-related differences were observed. At least three mice were used for each genotype at each age analyzed.

Genomic mapping. Homozygous *nm2719* mice were crossed to C3HeB/FeJ mice, and F1 heterozygotes were intercrossed to generate F2 mice. Genome scans were performed with polymorphic microsatellite markers (MIT markers) using genomic DNA collected from 15 affected and 15 unaffected F2 mice. For fine mapping, 1233 F2 mice were analyzed using MIT markers.

Immunohistochemistry. Mice were transcardially perfused with 10% neutral buffered formalin (NBF). Brains were dissected and postfixed in NBF for 3 h before paraffin embedding. To ensure equal processing, brains from a *Map1a* mutant mouse and an age-matched WT mouse were embedded in one block and sectioned onto the same slide. For immunofluorescence staining, deparaffinized slides were microwaved in antigen-retrieval buffer (10 mM Tris-HCl, pH 9.5, 2 mM EDTA, 0.05% Tween 20, for mouse anti-PSD-93 and goat anti-LC1 antibodies; 10 mM sodium citrate buffer, pH 6.0, for other antibodies) three times for 2 min each, separated by 10–15 min. Sections were then blocked with 4% goat serum in PBST (PBS with 0.05% Tween 20) for 30 min at room temperature and incubated with primary antibodies at 4°C overnight. Fluorescent detection was achieved with Alexa Fluor 488-conjugated and Alexa Fluor 555-conjugated secondary antibodies (Invitrogen). Fluorescent images were collected on a Leica SP5 confocal microscope (Leica Microsystems) and identical imaging conditions were applied to paired WT and mutant samples. For colorimetric calbindin D-28 staining, Bouin's fixative was used for perfusion and postfixation, and biotin-conjugated anti-rabbit IgG (Sigma-Aldrich), ExtrAvidin-peroxidase (Sigma-Aldrich), and 3,3′-diaminobenzidine (Sigma-Aldrich) were used for antibody detection. The primary antibodies used were as follows: rabbit anti-calbindin D-28 (CB-38a, Swant), rabbit anti-PKCγ (ab71558, Abcam), goat anti-MAP1A (N-18; specific for the N terminus of MAP1A-HC; sc-8969, Santa Cruz Biotechnology), mouse anti-MAP1 (specific for the C terminus of MAP1A-HC; clone HM-1, M4278, Sigma-Aldrich), rabbit anti-Myc (ab9106, Abcam), mouse anti-α-tubulin (clone B-5-1-2, T6074, Sigma-Aldrich), mouse anti-β-tubulin (clone TUB 2.1, SC-58886, Santa Cruz Biotechnology), mouse anti-βIII-tubulin (clone 2G10, ab78078, Abcam), mouse anti-acetylated α-tubulin (clone 6-11b-1, T6793, Sigma-Aldrich), mouse anti-polyglutamylated α-tubulin (clone B3, T9822, Sigma-Aldrich), mouse anti-tyrosinated α-tubulin (clone TUB-1A2, T9028, Sigma-Aldrich), rabbit anti-Δ2 α-tubulin (AB3203, EMD Millipore), mouse anti-MAP1B (clone 6; specific for the MAP1B heavy chain; sc-135978, Santa Cruz Biotechnology), goat anti-MAP1B (C-20; specific for the MAP1B light chain, LC1; sc-8971, Santa Cruz Biotechnology), mouse anti-MAP2 (clone HM-2, M9942, Sigma-Aldrich), mouse anti-PSD-93 (clone N18/28, University of California Davis/NIH NeuroMab Facility), mouse anti-Ankyrin G (clone N106/36, University of California Davis/NIH NeuroMab Facility), guinea pig anti-VGlut2 (AB5907, EMD Millipore) and rabbit anti-mGluR1a (445870; Calbiochem, EMD Millipore).

Histology. Sections from brains fixed with Bouin's fixative were stained with hematoxylin and eosin and cresyl violet according to standard protocols. Molecular layer thickness was measured in midsagittal sections along the III, IV, V, and VI lobules (midway down the adjoining fissures) as previously described (Borghesani et al., 2000). Measurements were averaged from three sections from three mice of each genotype.

Western blotting. Tissues were lysed in RIPA lysis buffer supplemented with Complete Protease Inhibitor Cocktail (Roche). Protein concentration was determined using Direct Detect Assay-free Cards and a Direct Detect Spectrometer (EMD Millipore). SDS-PAGE was performed using standard techniques. Primary antibodies (listed above) were detected with (1) anti-mouse HRP-conjugated secondary antibody (Bio-Rad), (2) anti-rabbit HRP-conjugated secondary antibody (Bio-Rad), or (3) anti-goat HRP-conjugated secondary antibody (Santa Cruz Biotechnology). SuperSignal West Pico Chemiluminescent Substrate (Pierce) was used for signal development. Rabbit anti-GAPDH antibody (Cell Signaling Technology) or HRP-conjugated β-actin antibody (Cell Signaling Technology) were included as loading controls.

Statistics. Results are mean ± SEM. Statistical significance was determined by unpaired *t* tests. p values <0.05 were considered significant.

Results

The *nm2719* mutation causes cerebellar Purkinje cell degeneration

The *nm2719* mutation arose spontaneously in a C57BLKS/J-*Npc1*^{spm} mouse colony and was segregated from the *Npc1*^{spm} mutation by a series of backcrosses to C57BLKS/J mice. Mice homozygous for the *nm2719* mutation (*nm2719*$^{-/-}$) developed

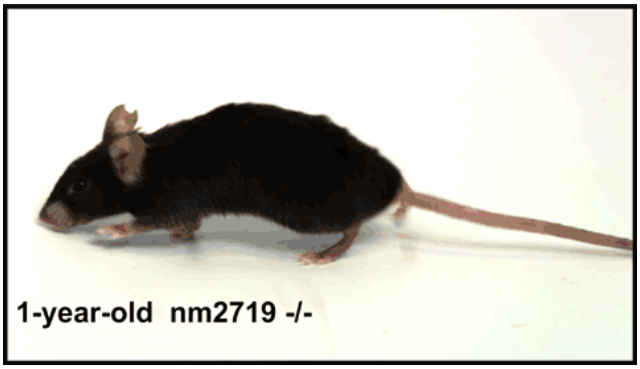

Movie 1. Locomotor deficits in 1-year-old *nm2719*$^{-/-}$ mice. A representative 1-year-old *nm2719*$^{-/-}$ mouse exhibited mild ataxia and tremors.

mild ataxia and tremors at 1 year of age, while heterozygous mice were indistinguishable from WT mice (Movie 1; data not shown).

Immunohistochemistry with antibodies to calbindin D-28 revealed that Purkinje cells in the *nm2719*$^{-/-}$ cerebellum developed axonal torpedoes, a hallmark of dystrophic axons, beginning at 6 weeks of age (Fig. 1*B*; data not shown), although loss of Purkinje cell soma was not observed before 3 months of age (Fig. 1*A–C*). However, patchy calbindin D-28 immunostaining indicative of Purkinje cell loss was observed in the mutant cerebellar cortex at 7 months of age, and by 18 months many Purkinje cells had degenerated in the mutant cerebellum (Fig. 1*D–L*). Loss of Purkinje cells in regions lacking calbindin staining in the *nm2719*$^{-/-}$ cerebellum was further confirmed by cresyl violet stain (Fig. 1*F*,*I*,*L*). Consistent with Purkinje cell loss, the thickness of the mutant molecular layer was reduced by 34% at 18 months of age (*nm2719*$^{-/-}$, 103.2 ± 3.378 μm; WT, 155.2 ± 1.922 μm, $n = 3$ for each genotype; $p < 0.0002$). Purkinje cell death was not observed in the cerebellum of aged *nm2719* heterozygous mice nor was neuronal death or reactive gliosis observed in noncerebellar regions of the homozygous mutant brain (data not shown).

The nm2719 mutation disrupts the mouse *Map1a gene*

The *nm2719* mutation was initially mapped to Chromosome 2 by a genome-wide scan of F2 mice from *nm2719* × C3HeB/FeJ crosses with MIT markers. Fine mapping further narrowed the critical region of the mutation to a 0.08 centimorgan interval (1.18 MB) containing 32 protein-coding genes (Fig. 2*A*). Genes within the critical interval were examined by cDNA sequencing, and a frameshift mutation (8 nt deletion and 1 nt insertion) was identified at nucleotides 5985–5992 of the *Map1a* open reading frame (Fig. 2*B*). This mutation was predicted to cause both a deletion of 297 aa from the C terminus of the MAP1A-HC and loss of the entire LC2 light chain, which are generated from proteolytic cleavage of the MAP1A precursor protein (Fig. 2*B*).

To confirm disruption of MAP1A in *nm2719* mutant mice, we performed Western blot analysis using an antibody specific to the C terminus of MAP1A-HC. This antibody detected a single high-molecular-weight band in the WT, but not the *nm2719*$^{-/-}$, brain (Fig. 2*C*). In addition, no bands were detected in brain extracts from *Map1a* knock-out mice (*Map1a*$^{tm1.2/tm1.2}$, hereafter referred to as *Map1a*$^{-/-}$), in which exon 5, encoding ~90% of the MAP1A precursor protein (Fig. 2*B*), was deleted. Western analysis with polyclonal antibodies raised against the N terminus of MAP1A-HC detected a faster migrating band in *nm2719*$^{-/-}$ brain extracts that was not present in WT or *Map1a*$^{-/-}$ samples, consistent with the prediction that *nm2719* mutation caused C-terminal truncation of MAP1A-HC (Fig. 2*C*).

Heterozygous *nm2719* mice do not have cerebellar defects, which suggests that expression of the truncated MAP1A protein does not cause disease, but rather that the pathology in *nm2719*$^{-/-}$ mice was due to loss of MAP1A function. To test this hypothesis, we performed calbindin D-28 immunohistochemistry and cresyl violet staining on cerebellar sections of *Map1a*$^{-/-}$ mice and on *nm2719* and *Map1a* compound heterozygous (*nm2719*$^{-}$/*Map1a*$^{-}$) mice. As observed in the *nm2719*$^{-/-}$ mice, Purkinje cell degeneration was apparent in mice of both genotypes by 7 months of age, and death of other neurons was not observed (Fig. 2*D*; data not shown). To further confirm that the cerebellar defects observed in *nm2719* mutant mice are due to loss of *Map1a*, we performed an *in vivo* complementation assay in which transgenic mice expressing *Map1a* from a WT cosmid (Ikeda et al., 2002) were crossed with *nm2719* mutant mice. Neither locomotor defects nor Purkinje cell loss was observed in the resulting TgMap1a; *nm2719*$^{-/-}$ offspring, even at 18 months of age (Fig. 2*E*; data not shown). Together these results demonstrate that loss of the C-terminal region of MAP1A-HC and/or LC2 causes Purkinje cell degeneration in aged mice.

Both MAP1A-HC and LC2 can bind to MTs (Langkopf et al., 1992; Cravchik et al., 1994; Chien et al., 2005). Therefore, to determine whether LC2 expression was sufficient to rescue Purkinje cell loss in the *nm2719*$^{-/-}$ cerebellum, we generated transgenic mice using a construct in which LC2 (epitope tagged with Myc) was placed downstream of the NSE promoter (TgLC2; Fig. 2*F*; Twyman and Jones, 1997). Although LC2 was expressed in transgenic Purkinje cells as indicated by immunofluorescence with Myc antibodies, calbindin D-28 immunohistochemistry and cresyl violet staining revealed that these neurons still degenerated in the TgLC2; *nm2719*$^{-/-}$ cerebellum (Fig. 2*F*; data not shown), suggesting that the C-terminal domain of MAP1A-HC is essential for Purkinje cell survival.

Reduction in the MT network in *Map1a* mutant Purkinje cells

MAP1A directly binds to MTs, forming elaborate cross-bridges between MTs and/or MTs and other cellular structures in neuronal dendrites (Shiomura and Hirokawa, 1987a). In addition, expression of MAP1A has been shown to increase MT stability in cultured cells (Vaillant et al., 1998). In the cerebellum, MAP1A is highly enriched in the somatodendritic region of adult Purkinje cells (Huber and Matus, 1984b), as shown by its colocalization with PKCγ, a protein kinase C isoform specifically expressed in Purkinje cells in the cerebellum (Fig. 3*A*). To determine whether MAP1A deficiency alters the MT network in Purkinje cells, immunofluorescence analysis for both α-tubulin and β-tubulin was performed on WT and *Map1a*$^{-/-}$ cerebellar sections. Indeed, both tubulin isoforms were specifically reduced in the soma and, to a lesser extent, the dendritic shaft of *Map1a* mutant Purkinje cells at postnatal day (P) 18 (Fig. 3*B*,*C*), a time when maximum levels of MAP1A are reached in the brain (Riederer and Matus, 1985). Notably, both tubulin isoforms remain unchanged in mutant parallel fibers, which densely fill the molecular layer surrounding Purkinje cell dendrites. Similarly, β III-tubulin (TUJ1), a neuronal-specific isoform of β tubulin, was also reduced in *Map1a*$^{-/-}$ Purkinje cells (Fig. 3*D*). These tubulin isoforms exhibited fibrous structures under high magnification in both WT and mutant Purkinje cell soma (Fig. 3*B–D*, insets), typical of polymerized MT networks. These results suggest that loss of *Map1a* results in a decrease in MT networks in Purkinje cells.

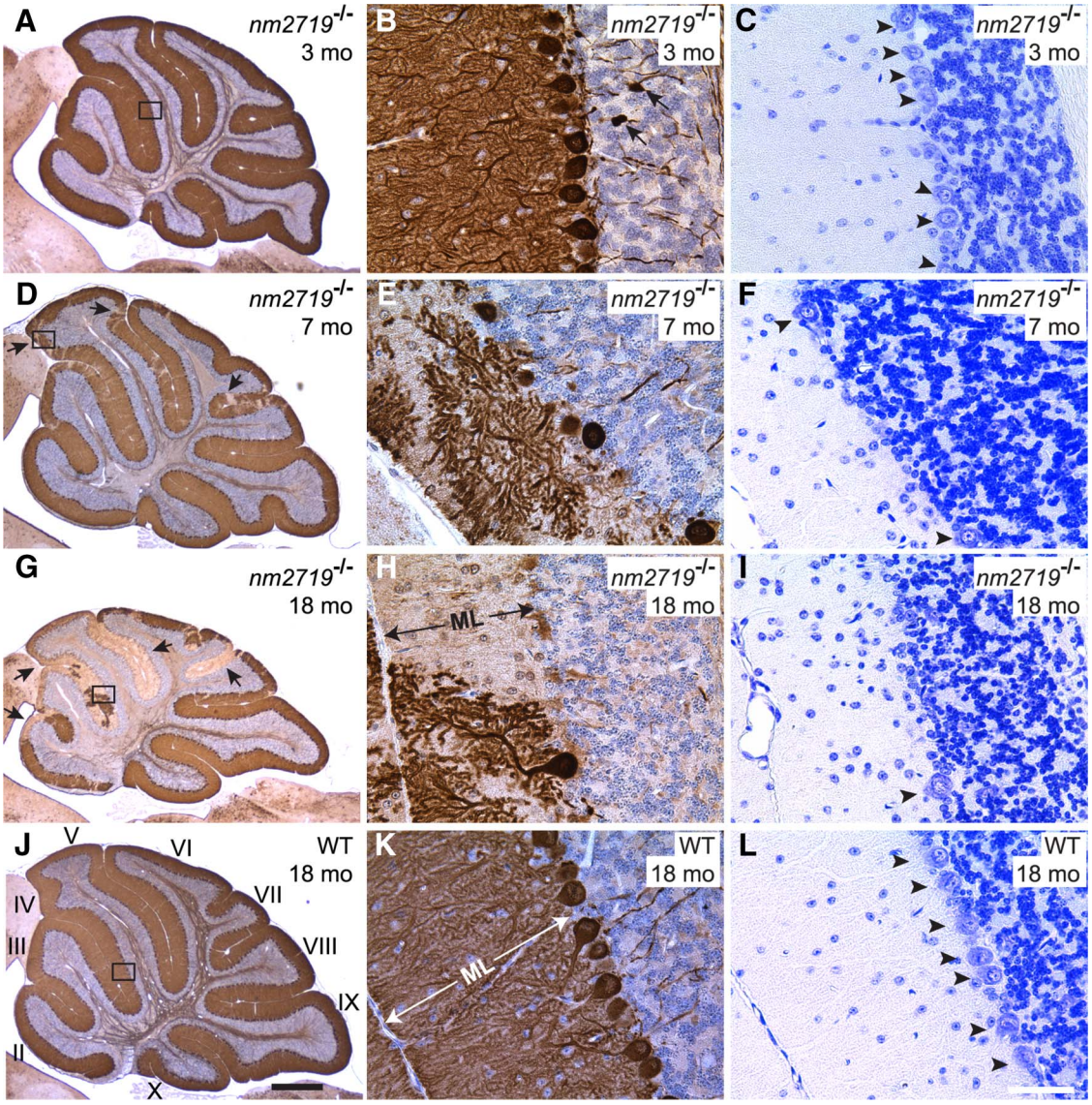

Figure 1. Degeneration of Purkinje cells in *nm2719* $^{-/-}$ mice. ***A***, ***D***, ***G***, ***J***, Calbindin D-28 immunohistochemistry (brown) on cerebellar sections from 3-month-old (***A***), 7-month-old (***D***), and 18-month-old (***G***) *nm2719* $^{-/-}$ and 18-month-old WT (***J***) mice. Arrows point to areas with patchy Purkinje cell loss. ***B***, ***E***, ***H***, ***K***, Higher-magnification images of boxed areas in the left panels. Arrows point to focal swellings in dystrophic Purkinje cell axons. ***C***, ***F***, ***I***, ***L***, Comparative regions of the middle panels in neighboring sections (14 μm away) stained with cresyl violet to visualize Purkinje cell soma (arrowheads). Note the loss of Purkinje cell soma in the 7-month-old (***F***) and the 18-month-old (***I***) *nm2719* $^{-/-}$ cerebellum, but not in the 3-month-old (***C***) *nm2719* $^{-/-}$ cerebellum or in the WT (***L***) cerebellum. Lobules are indicated by Roman numerals (***J***). ML, Molecular layer. Scale bars: ***J***, 500 μm; ***L***, 50 μm.

Tubulin is subject to many post-translational modifications (PTMs) that affect MT stability, the association of MTs with MAPs, and MT function (Janke and Bulinski, 2011). Thus we explored whether decreased levels of tubulins in *Map1a* mutant Purkinje cells were the result of reduction in MTs with different PTMs. Except for glycylated and detyrosinated tubulin, most tubulin PTMs have been detected in the somatodendritic domain of mature Purkinje cells (Cambray-Deakin and Burgoyne, 1987; Paturle-Lafanechère et al., 1994; Iftode et al., 2000; Ikegami et al., 2007). Immunofluorescence for acetylated and Δ2 α-tubulin, which both exist in stable long-lived MTs (Wloga and Gaertig, 2010; Janke and Bulinski, 2011), revealed that both subtypes were reduced in the soma of *Map1a* $^{-/-}$ Purkinje cells (Fig. 3*E*; data not shown). Additionally, a similar reduction was observed in polyglutamylated α-tubulin (Fig. 3*F*), a PTM that regulates interactions of MTs with MAP1A and other MAPs (Bonnet et al., 2001; Janke et al., 2008). However, no differences were observed between WT and *Map1a* mutant Purkinje cells for tyrosinated α-tubulin (Tyr-tub; Fig. 3*G*), the unmodified tubulin that is often associated with newly polymerized unstable MTs or with retyrosination of depolymerized tubulin (Janke and Bulinski, 2011). Notably, higher levels of Tyr-tub were observed along the peripheral dendritic shaft of both mutant and WT Purkinje cells, indicating that this tubulin subtype may not be incorporated into the stable dendritic MT network, but exists in the soluble tubulin pool or in highly dynamic MTs (Fig. 3*H*). In contrast, tubulins with other PTMs displayed a centralized distribution along the dendritic shaft of Purkinje cells of both genotypes, as expected by their association with MTs (Fig. 3*I*; data not shown). The reduction of the MT network persisted in Purkinje cells of aged *Map1a* mutant mice and was limited to these neurons (data not shown).

Decreases in Purkinje cell somatodendritic MTs occurred long before neuron death in the *Map1a* mutant cerebellum, suggesting that MT changes are a direct consequence of MAP1A

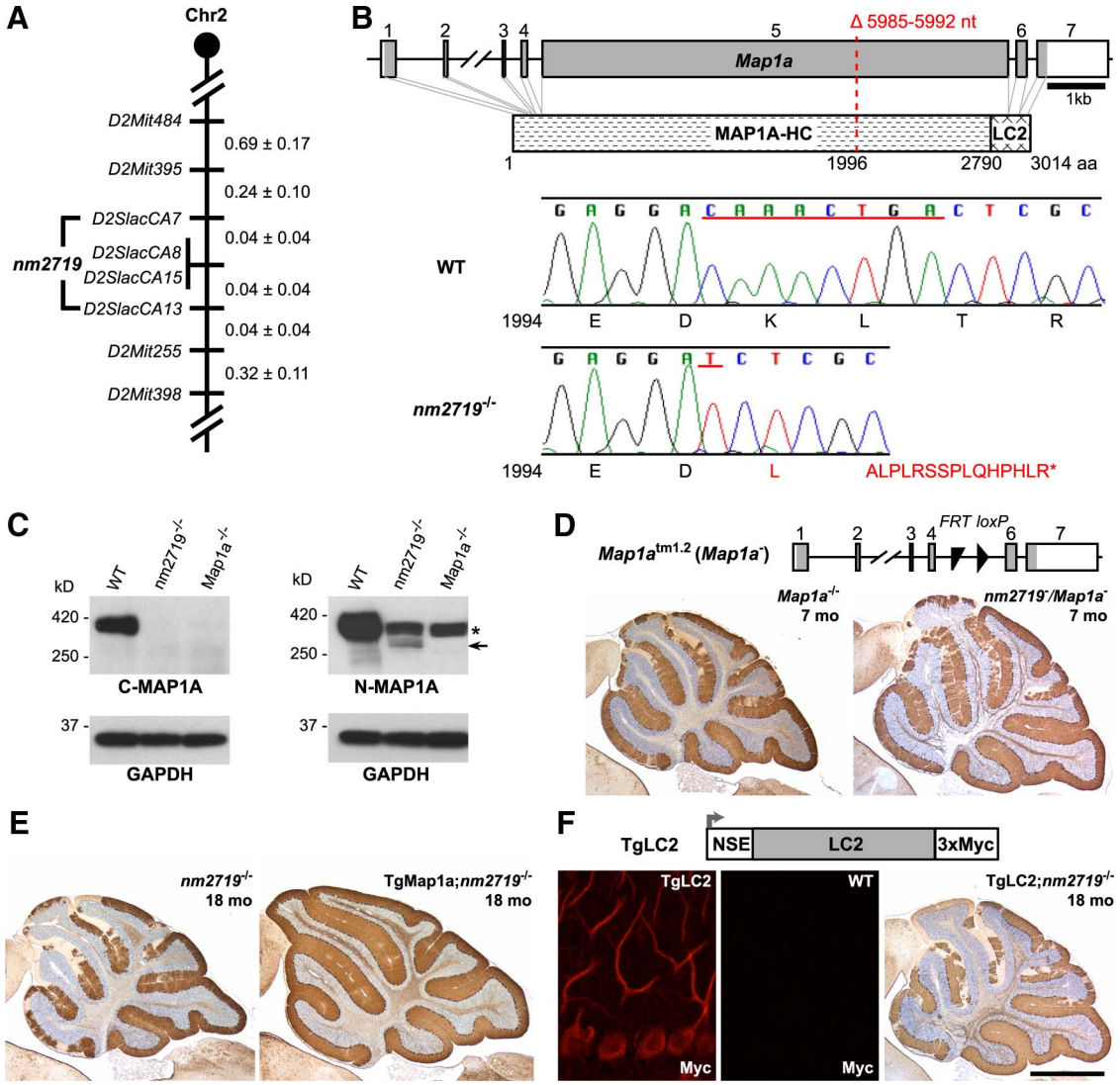

Figure 2. The *nm2719* mutation disrupts *Map1a* gene. ***A***, Mapping of the *nm2719* mutation on chromosome 2 (shown in centimorgans ± SEM). ***B***, The *nm2719* mutation in the *Map1a* gene (top; open reading frame is shaded) and protein (middle). The 8 nt deletion and 1 nt insertion are underlined on the sequencing chromatograms of WT and *nm2719* $^{-/-}$ cDNA, respectively. Encoded amino acids (*, stop codon) are shown at the bottom of each chromatogram. ***C***, Western analysis of WT, *nm2719* $^{-/-}$, and *Map1a* $^{-/-}$ brain lysates with antibodies to the C terminus (C-MAP1A, left) or the N terminus (N-MAP1A, right) of MAP1A-HC. An arrow indicates the truncated form of MAP1A-HC found only in the *nm2719* $^{-/-}$ brain. The N-terminal antibody also recognizes a nonspecific band (asterisk) across all genotypes, which is likely to be MAP1B given the similar molecular weight and high-sequence homology in this domain between MAP1A and MAP1B. ***D***, Purkinje cell loss in *Map1a* knock-out mice. Schematic of the *Map1a* knock-out allele (top). Calbindin D-28 immunohistochemistry (IHC) on 7-month-old *Map1a* $^{-/-}$ and *nm2719* $^{-/-}$*/Map1a* $^{-}$ cerebellar sections. ***E***, Neuron death was rescued by the *Map1a* transgene as shown by calbindin D-28 IHC on 18-month-old *nm2719* $^{-/-}$ and TgMap1a; *nm2719* $^{-/-}$ cerebellar sections. ***F***, Transgenic expression of LC2 failed to rescue neuron loss in *nm2719* $^{-/-}$ mice. Schematic of the transgene is shown and Purkinje cell expression of the transgene was confirmed by Myc immunofluorescence on 2-month-old WT and TgLC2 cerebella. Calbindin D-28 IHC on a representative cerebellar section from 18-month-old TgLC2; *nm2719* $^{-/-}$ mice is shown. Scale bar, 1 mm.

deficiency rather than a general phenomenon associated with dying Purkinje cells. To test the hypothesis, we performed immunofluorescence analysis of the above-mentioned tubulin isoforms and PTMs in a different Purkinje cell degeneration model, the vacillator (*vac*) mutant mouse, which has mutation in the gene encoding calcineurin B homologous protein 1 (CHP1), an essential cofactor for a family of sodium hydrogen exchangers (NHEs). *Chp1*^{vac} likely causes Purkinje cell death by disrupting the plasma membrane localization and ion exchange activity of NHEs (Liu et al., 2013). Indeed, all tubulin isoforms and subtypes examined were at similar levels in *Chp1*$^{vac/vac}$ and WT Purkinje cells at P18 and 2 months of age (Fig. 3*J*,*K*; data not shown), implying reduced MTs are not necessarily associated with degenerative Purkinje neurons. Similarly, no changes in MT levels were discovered in mice homozygous for the sticky mutation (data not shown), which disrupts the editing domain of the alanyl-tRNA synthetase and causes Purkinje cell death through compromising translational fidelity (Lee et al., 2006). Together these observations suggest that MAP1A deficiency specifically causes reductions in somatodendritic MTs of Purkinje cells before cell death.

In addition to MAP1A, MAP1B and MAP2 are also expressed in adult Purkinje cells (Huber and Matus, 1984a; Schoenfeld et al., 1989). To determine whether loss of MAP1A and reductions in MT networks in mutant Purkinje cells affect the level of these structural MAPs, we performed Western blot analysis using cerebellar extracts from 2-month-old WT, *nm2719* $^{-/-}$, and *Map1a* $^{-/-}$ mice. Similar levels of MAP1B heavy chain (MAP1B-HC; hereafter referred to as MAP1B), MAP1B light chain (LC1), and MAP2 were detected in all genotypes, which suggests that

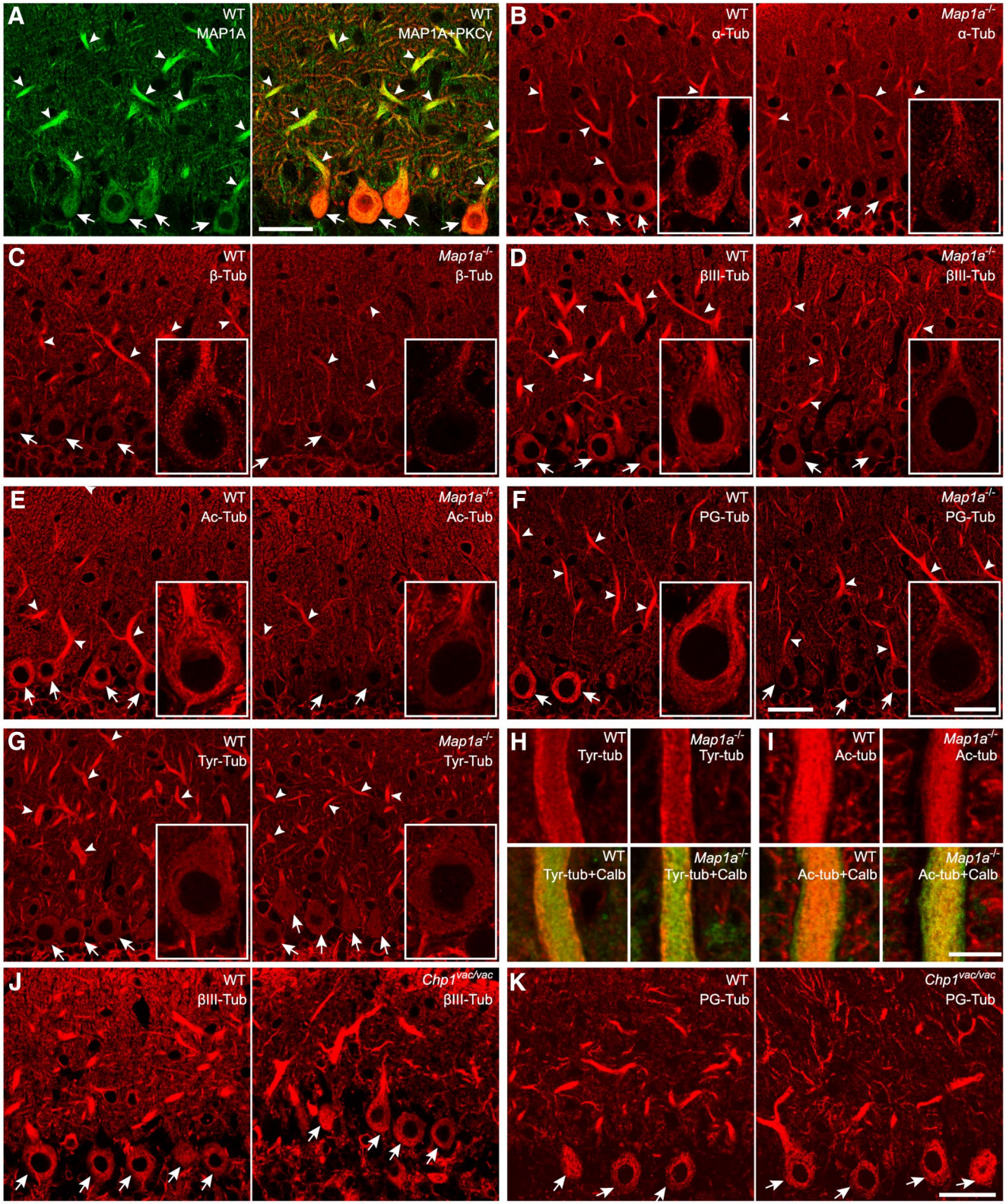

Figure 3. Reduced MT networks in the *Map1a* $^{-/-}$ Purkinje cell somatodendritic region. ***A***, MAP1A-HC localization in the soma (arrows) and dendrites (arrowheads) of WT Purkinje cells at P18, revealed by coimmunofluorescence (IF) for MAP1A-HC (C-terminal antibody; green) and PKCγ (red). ***B–G***, IF staining for α-tubulin (α-Tub, ***B***), β-tubulin (β-Tub, ***C***), β IIII-tubulin (βIII-Tub, ***D***), acetylated tubulin (Ac-tub, ***E***), polyglutamylated tubulin (PG-tub, ***F***), or Tyr-tub (***G***) on cerebellar sections from P18 WT (left) and *Map1a* $^{-/-}$ (right) mice. Insets, Higher-magnification images of representative Purkinje cell soma. Note all tubulin isoforms or subtypes except for Tyr-tub were reduced in the soma (arrows) of mutant Purkinje cells. Reduction of α-Tub and β-Tub was also observed along the dendritic shaft (arrowheads). ***H***, Co-IF staining for Tyr-tub (red, top) and calbindin D-28 (green; merged images, bottom) showed the enrichment of Tyr-tub along the peripheral dendritic shaft of both WT (left) and *Map1a* $^{-/-}$ (right) Purkinje cells at P18. ***I***, Co-IF staining for Ac-tub (red) and calbindin D-28 (green; merged images, bottom) showed high Ac-tub signals in the center of the WT (left) and the *Map1a* $^{-/-}$ (right) Purkinje cell dendritic shaft at P18. ***J***, ***K***, No differences in βIII-Tub (***J***) and PG-tub (***K***) levels were observed between *Chp1* $^{vac/vac}$ and WT Purkinje cells at P18. Arrows point to Purkinje cell soma. Identical staining and imaging conditions were used for all WT and mutant pairs of sections. Scale bars: ***A***, ***F***, ***K***, 30 μm; ***F*** inset, 10 μm; ***I***, 5 μm.

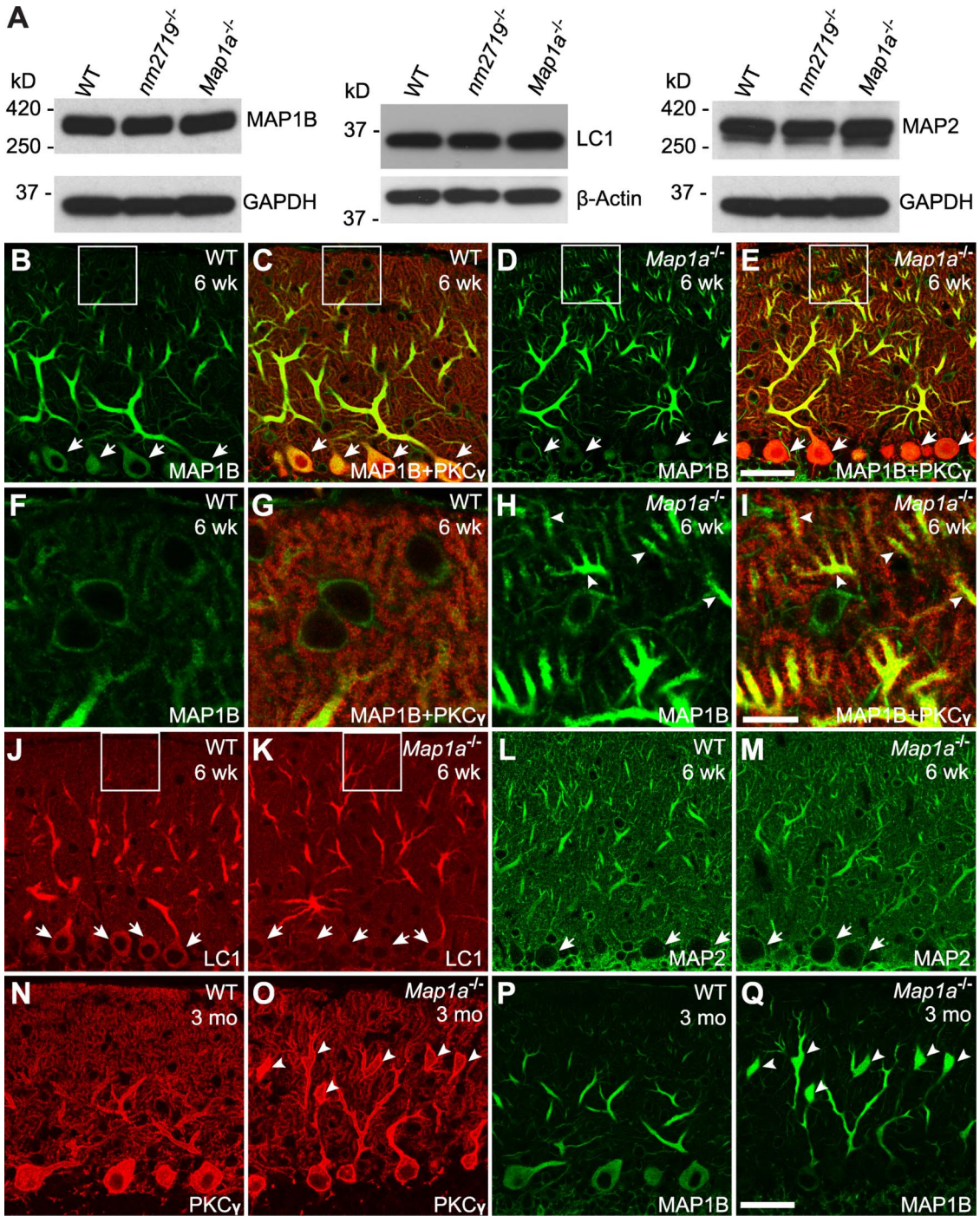

Figure 4. Aberrant somatodendritic distribution of the MAP1B heavy and light chains in *Map1a* $^{-/-}$ Purkinje cells. ***A***, Western blot analysis for MAP1B, LC1, and MAP2 using WT, *nm2719* $^{-/-}$, and *Map1a* $^{-/-}$ cerebellar lysates. No change in protein abundance was detected across different genotypes. GAPDH or β-actin included as loading controls. ***B–E***, Coimmunofluorescence (IF) staining for MAP1B (green; ***B–E***) and PKCγ (red; merged images, ***C***, ***E***) on cerebellar sections from 6-week-old WT and *Map1a* $^{-/-}$ mice. Note reduced MAP1B in Purkinje cell soma (***D***, arrows). ***F–I***, Higher-magnification images of boxed areas in ***B–E***. Note increased MAP1B signals in distal dendrites (***H***, arrowheads) of *Map1a* $^{-/-}$ Purkinje cells. ***J–M***, IF staining for LC1 (***J***, ***K***) and MAP2 (***L***, ***M***) on WT (***J***, ***L***) and *Map1a* $^{-/-}$ (***K***, ***M***) cerebellar sections. Arrows indicate Purkinje cell soma. ***N–Q***, Co-IF staining for PKCγ (***N***, ***O***) and MAP1B (***P***, ***Q***) on cerebellar sections from WT (***N***, ***P***) and *Map1a* $^{-/-}$ (***O***, ***Q***) mice. Arrowheads point to focal swellings in *Map1a* $^{-/-}$ Purkinje cell dendrites. Identical staining and imaging conditions were used for all WT and mutant pairs of sections. Scale bars: ***B–E***, ***J–Q***, 40 μm; ***I***, 10 μm.

disruption of MAP1A did not change the overall abundance of these MAPs in the cerebellum (Fig. 4*A*).

To investigate whether the subcellular distribution of MAP1B, LC1, or MAP2 was affected by loss of MAP1A, immunofluorescence was performed on cerebellar sections from 6-week-old WT and *Map1a* $^{-/-}$ mice. Similar to MAP1A and tubulins, the highest levels of MAP1B were observed in the proximal dendritic shaft of WT Purkinje cells, while lower levels were found in the soma and distal dendritic branches in the outer molecular layer (Fig. 4*B*,*C*). In *Map1a* $^{-/-}$ Purkinje cells, however, MAP1B was greatly diminished in Purkinje cell soma, while its level in the proximal dendritic shaft remained relatively unchanged (Fig. 4*D*,*E*). In

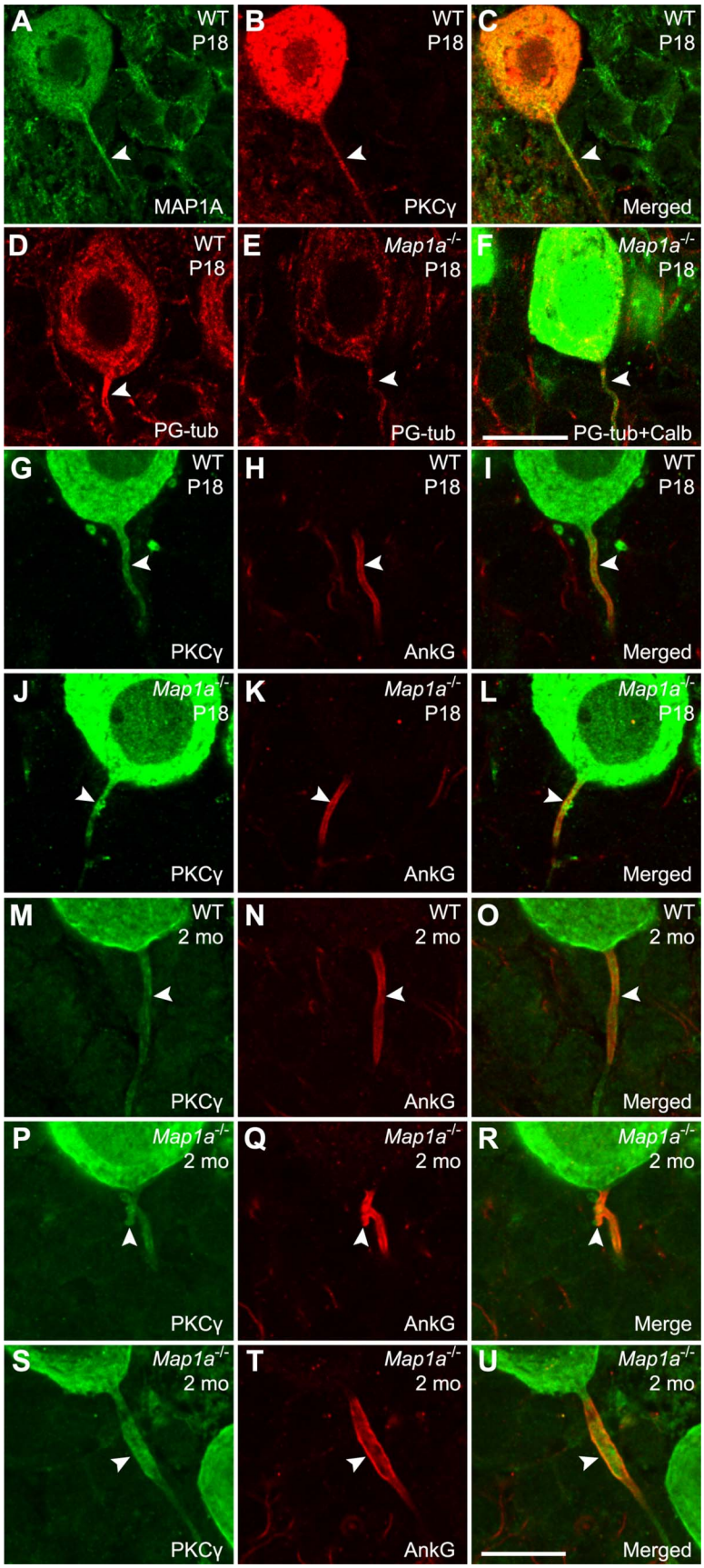

Figure 5. Loss of MAP1A disrupts the axon initial segment of Purkinje cells. ***A–C***, MAP1A localization at the AIS of Purkinje cells as shown by coimmunofluorescence (IF) with antibodies to MAP1A and PKCγ on P18 WT cerebellar sections. ***D–F***, Co-IF with antibodies to polyglutamylated-tubulin (PG-tub) and calbindin D-28 (Calb) on P18 WT (***D***) and *Map1a* $^{-/-}$ cerebellar sections (***E***, ***F***). Note the reduced levels of PG-tub at the AIS of *Map1a* $^{-/-}$ Purkinje cells (***E***, arrowheads). ***G–I***, Co-IF with antibodies to PKCγ and ankryrin G (AnkG) on cerebellar sections from P18 WT (***G–I***) and *Map1a* $^{-/-}$ (***J–L***) Purkinje cells. No defects were observed in the AIS of *Map1a* $^{-/-}$ Purkinje cells at this age. ***M–U***, Co-IF with antibodies to PKCγ and AnkG on cerebellar sections from 2-month-old WT (***M–O***) and *Map1a* $^{-/-}$ (***P–U***) mice. Note the blebbing (***P–R***, arrowheads) and hypertrophy (***S–U***, arrowheads) in the mutant AIS. Arrowheads indicate the AIS of Purkinje cells. Identical staining and imaging conditions were applied to all WT and mutant pairs of sections. Scale bars: ***A–F***, 15 μm; ***G–U***, 10 μm.

addition, abnormally high levels of MAP1B were observed in the distal dendritic segments of mutant Purkinje cells (Fig. 4*F–I*). Similarly, LC1 was reduced in the soma and increased in distal dendritic branchlets of *Map1a* $^{-/-}$ Purkinje cells (Fig. 4*J*,*K*). In contrast to MAP1B and LC1, no obvious differences in the dendritic or soma localization of MAP2 were observed between *Map1a* $^{-/-}$ and WT Purkinje cells (Fig. 4*L*,*M*). Like tubulins, no changes in the level or subcellular distribution of MAP1B or LC1 were observed in other neurons in the *Map1a*-deficient murine brain (data not shown). The abnormal distribution of MAP1B and LC1 in the soma and distal dendritic arbors of *Map1a* mutant Purkinje cells further supports the notion that MAP1A has a critical role in modulating the proper organization of neuronal MT networks in the somatodendritic compartment.

In addition, immunofluorescence using antibodies to calbindin D-28 or PKCγ revealed abnormal focal swellings in *nm2719* $^{-/-}$ and *Map1a* $^{-/-}$ Purkinje cell dendrites beginning at 6 weeks of age (data not shown). These abnormalities became more widespread with age (Fig. 4*N*,*O*). Immunofluorescence with antibodies to MAP1B, LC1, α-tubulin, and β-tubulin demonstrated that these proteins accumulated within such dendritic swellings (Fig. 4*P*,*Q*; data not shown). Together, our data suggest that MAP1A is important for the maintenance of dendritic MT structures that are pivotal for the normal dendritic morphology of Purkinje cells.

Map1a is necessary for the maintenance of the Purkinje cell AIS

Although MAP1A, MAP1B, and MAP2 are present in the soma and dendrites of Purkinje cells, MAP1A is the only MAP that is highly enriched in the AIS (Huber and Matus, 1984b; Fig. 5*A–C*), which is a specialized axon structure where action potentials are initiated and fascicles of MTs reside (Palay et al., 1968). Notably, no im-

munofluorescence signal for MAP1A was detected in the white matter of the adult cerebellum, through which axons of Purkinje cells descend (data not shown). This suggests MAP1A is not localized to axons of Purkinje cells beyond the initial segment, which is consistent with a previous study (Szebenyi et al., 2005). Furthermore, immunofluorescence with antibodies to α-tubulin, β-tubulin, or β III-tubulin revealed levels of these proteins were decreased in the AIS of *Map1a* $^{-/-}$ Purkinje cells at P18 (data not shown). Similarly, polyglutamylated and acetylated tubulin, both of which are highly enriched at the Purkinje cell AIS, were reduced in this structure in *Map1a* $^{-/-}$ Purkinje cells (Fig. 5*D–F*; data not shown). Together, these data suggest that MAP1A deficiency also affects the MT network in the Purkinje cell AIS.

To determine whether MAP1A deficiency and the accompanying alterations in MT components resulted in morphological changes in the Purkinje cell AIS, immunofluorescence was performed on cerebellar sections from P18 *Map1a* $^{-/-}$ and WT mice using antibodies to the Purkinje cell marker PKCγ and ankyrin G, a master organizer and marker of AIS. At P18, just after Purkinje cell maturation, the AIS of *Map1a* $^{-/-}$ Purkinje cells were indistinguishable from that of WT neurons (Fig. 5*G–L*). However at 2 months of age, the AIS of many *Map1a* $^{-/-}$ Purkinje cells were hypertrophic or exhibited abnormal blebs in contrast to the smooth and slender AIS of WT Purkinje cells (Fig. 5*M–U*). Similar defects were observed in Purkinje cells of 2-month-old *nm2719* $^{-/-}$ mice (data not shown). As observed for Purkinje cell death, expression of LC2 was not sufficient to rescue the AIS defects in TgLC2; *nm2719* $^{-/-}$ Purkinje cells (data not shown), suggesting that the MAP1A-HC is required to preserve the proper structure of Purkinje cell AIS. Together, these results suggest that MAP1A-HC is required for the maintenance, but not the initial establishment, of the Purkinje cell AIS.

Reduced PSD-93 in *Map1a* mutant cerebellum

Previous studies have reported that a C-terminal domain of MAP1A-HC interacts with the guanylate kinase domain of the MAGUKs (Brenman et al., 1998; Reese et al., 2007). Of the four neuronal MAGUKs that are present in the mammalian brain, PSD-93 is the only member that is found in Purkinje cells and is localized to the surface membranes of dendritic spines and postsynaptic densities of these neurons. Additionally, PSD-93 is associated with MTs in the dendritic shafts of Purkinje cells, the primarily location of MAP1A and presumably the site of interaction of these molecules (Brenman et al., 1996; Kim et al., 1996; McGee et al., 2001). To determine whether MAP1A deficiency affects PSD-93 levels in the cerebellum, we performed Western blot analysis on WT, *nm2719* $^{-/-}$, and *Map1a* $^{-/-}$ cerebellar lysates using an antibody to PSD-93 (Fig. 6*A*). Indeed, PSD-93 levels were reduced in both the *nm2719* $^{-/-}$ and *Map1a* $^{-/-}$ cerebellum.

To further explore which subcellular localization of PSD-93 was affected in *Map1a*-deficient Purkinje cells, coimmunofluorescence for PSD-93 and calbindin D-28 was performed on cerebellar sections from 5-week-old WT and *Map1a* $^{-/-}$ mice. PSD-93 was greatly reduced in the soma and dendritic shafts of mutant Purkinje cells, suggesting that the MT localization of this protein was disrupted by MAP1A deficiency (Fig. 6*B–G*). In addition, PSD-93 signals were moderately decreased in broad areas of the molecular layer surrounding Purkinje cell dendritic shafts (Fig. 6*B*,*E*), presumably reflecting the reduction of the protein in dendritic spines of these neurons (Fig. 6*H–M*). Similar reductions in PSD-93 levels were observed in age-matched *nm2719* $^{-/-}$ Purkinje cells (data not shown). PSD-93 is localized to both the climbing fiber–Purkinje cell and parallel fiber–Purkinje cell synapse (Roche et al., 1999). To determine whether decreased PSD-93 in the somatodendritic compartment of mutant Purkinje cells is due to improper formation of climbing fiber–Purkinje cell synapses, we performed immunofluorescence with antibodies to vesicular glutamate transporter 2 (VGlut2), which is found at climbing fiber presynaptic terminals. As shown in Figure 6*N–Q*, no difference in this marker was observed between the WT and *Map1a* mutant cerebellum. Similarly, parallel fiber–Purkinje cell synapses were comparable between 5-week-old WT and *Map1a* mutant cerebellum by transmission electron microscopy (TEM) analysis (data not shown). Together these observations suggest that loss of MAP1A has a dramatic effect on the localization of PSD-93 along MTs in the somatodendritic compartment of Purkinje cells, which may contribute to decreased levels of the MAGUK in dendritic spines of these neurons.

Discussion

The structural MAPs are highly enriched in the mammalian brain. Although mutation studies have revealed important *in vivo* functions of tau, MAP2, and MAP1B, less is known about MAP1A (Meixner et al., 2000; Harada et al., 2002; Lei et al., 2012). Our results demonstrate that loss of MAP1A causes neuronal death. MAP1A is mainly localized to the soma and dendritic shafts of neurons. Indeed, we observed disturbance of MT organization in the somatodendritic domain of Purkinje cells before neurodegeneration. Our results pinpoint the critical role of this MAP in the proper organization of somatodendritic MT network, which in turn is important for neuronal survival.

A previous study showed that MAP1A is critical for activity-dependent dendritic branching and dendritic arbor stabilization in cultured neurons, although the specific mechanisms remain largely unknown (Szebenyi et al., 2005). Here we demonstrate that *Map1a* deficiency caused both a decrease in the density of the MT network and aberrant distribution of MAP1B in the somatodendritic compartment of Purkinje cells, suggesting the involvement of MAP1A in proper organization of somatodendritic MT network. Moreover, we show that multiple MT isoforms and PTMs were also reduced in mutant Purkinje cells, further illustrating the profound disturbance in MT organization. Notably, tryosinated tubulin, the tubulin subtype that is often found in highly dynamic MT or unpolymerized tubulin (Janke and Kneussel, 2010), was not changed by the *Map1a* mutation, supporting the notion that MAP1A specifically affects organization of stable MTs in neurons. MAP1A is unlikely to be directly involved in the very basic process of MT polymerization suggesting that this MAP may play a role in such processes as the modulation of tubulin PTM, fine-tuning of MT assembly, and maintenance of MT stability in the soma and dendrites of Purkinje cells. Furthermore, changes in somatodendritic MTs in *Map1a* mutant Purkinje cells are likely to be directly associated with MAP1A deficiency rather than a nonspecific process occurring during neurodegeneration, as MT alterations are observed long before cell death and are not observed in two other Purkinje cell-degenerative mouse models in which the mechanisms of disease are not relevant to the MT cytoskeleton. MT abnormalities may also contribute to neuron death. In agreement with this idea is the finding that the Purkinje cell degeneration (*pcd*) mutation that disrupts the gene encoding cytosolic carboxypeptidase 1 (*Ccp1*, also called *Agtpbp1* or *Nna1*), an enzyme that functions to remove Glu residues from the polyglutamyl side chains of α-tubulin and β-tubulin, causes degeneration of multiple neuronal types, including Purkinje cells (Mullen et al., 1976; Fernandez-Gonzalez et al., 2002; Rogowski et al., 2010; Berezniuk et al., 2012).

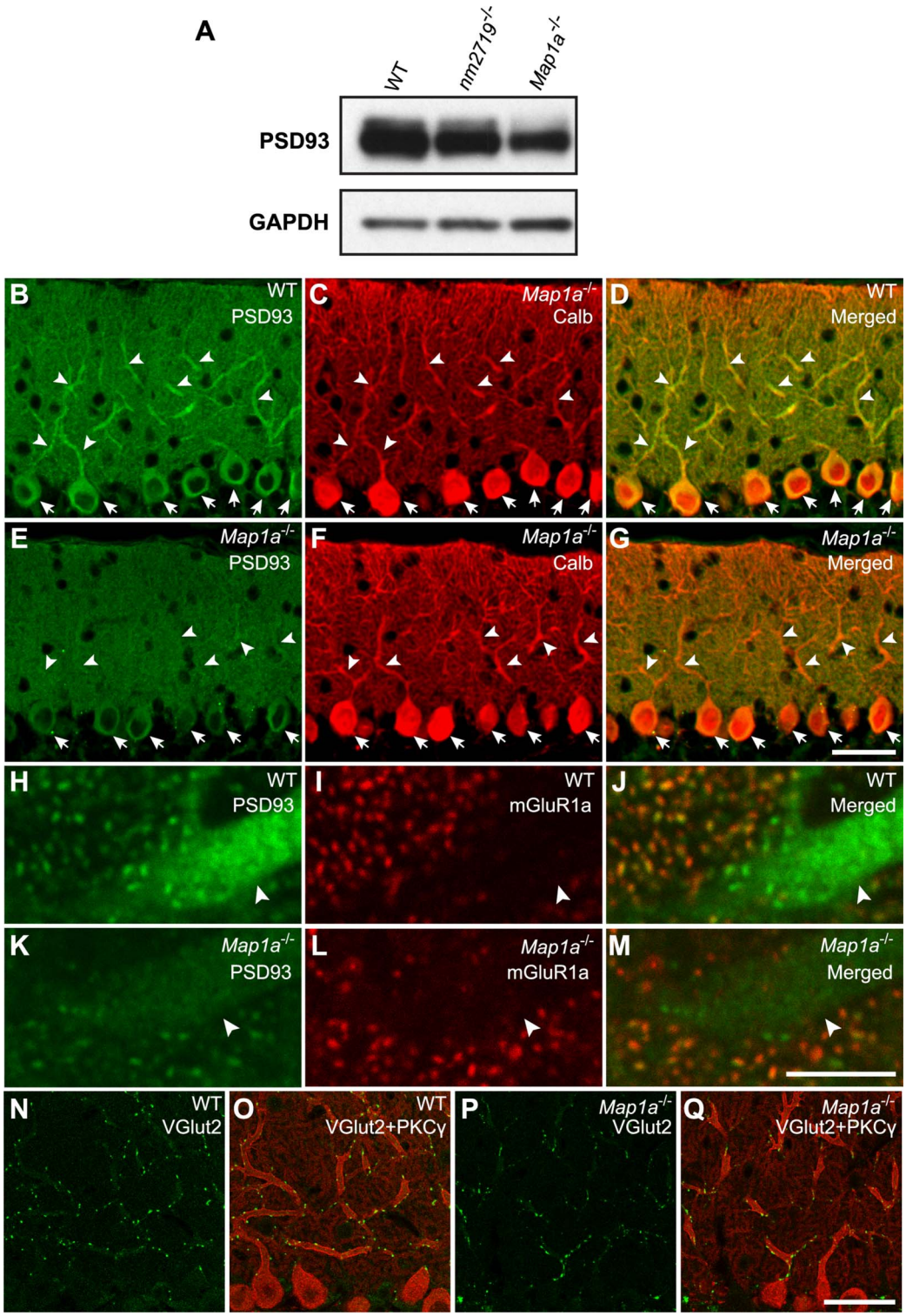

Figure 6. Loss of *Map1a* reduces PSD-93 levels in Purkinje cells. ***A***, Western blot analysis of WT, *nm2719* $^{-/-}$, and *Map1a* $^{-/-}$ cerebella using antibodies to PSD-93. GAPDH served as a loading control. ***B–G***, Coimmunofluorescence (Co-IF) on cerebellar sections from 5-week-old WT (***B–D***) and *Map1a* $^{-/-}$ (***E–G***) mice using antibodies to PSD-93 and calbindin D-28 (Calb). Note PSD-93 levels were dramatically reduced in the soma (arrows) and dendritic shafts (arrowheads) of *Map1a* $^{-/-}$ Purkinje cells. ***H–M***, Colocalization of PSD-93 and mGluR1a at dendritic spines of WT (***H–J***) and *Map1a* $^{-/-}$ (***K–M***) Purkinje cells by co-IF. Representative Purkinje cell dendritic shafts were indicated by arrowheads. Note the reduction of PSD-93 levels in dendritic spines of mutant Purkinje cells. ***N–Q***, Co-IF staining for VGlut2 (***N–Q***, green) and PKCγ (***O***, ***Q***, merged images, red) revealed climbing fiber–Purkinje cell synapses in 5-wk-old WT (***N***, ***O***) and *Map1a* $^{-/-}$ (***P***, ***Q***) cerebella. No differences in staining were observed between the two genotypes. Identical staining and imaging conditions were used for all WT and mutant pairs of sections. Scale bars: ***G***, 50 μm; ***M***, 5 μm; ***Q***, 40 μm.

The specificity of neuronal defects in the *Map1a*-deficient mouse may be due to functional redundancy among the structural MAPs. Although *Map1a*, *Map1b*, and *Map2* display distinct temporal and spatial expression patterns, these proteins also colocalize, especially in the somatodendritic compartment, of many neurons in the brain (Huber and Matus, 1984a; Shiomura and Hirokawa, 1987b; Schoenfeld et al., 1989). For example, heterozygosity for a potential dominant negative allele of *Map1b*

resulted in developmental defects in dendritic growth and branching of Purkinje cells (Edelmann et al., 1996). Interestingly, MAP1A, but not MAP2, was reduced in Purkinje cells of these mice. Given that dendritic growth and branching of Purkinje cells were not disrupted in either complete *Map1b* knock-out mice (Meixner et al., 2000) or in our *Map1a* mutant strains (Y. Liu and S. L. Ackerman, unpublished observations), it is likely that MAP1A and MAP1B function cooperatively to modulate Purkinje cell dendritic arborization. Similar synergy exists between MAP1B and MAP2 in dendritic development of cultured hippocampal neurons (Teng et al., 2001). In addition to modulating dendritic structure, functional redundancy of MAP1A, MAP1B, and MAP2 may also underlie the specific degeneration of Purkinje cells in *Map1a* mutant mice. Generation of *Map1a* mutant mice that are also deficient in *Map2* or *Map1b* could lead to a broader, and more severe, spectrum of neuron defects and would test the genetic redundancy of these MAPs.

MAP1A, besides being highly enriched in the somatodendritic compartment, is also highly enriched in the AIS of Purkinje cells in the adult cerebellum. However, unlike other AIS cytoskeletal proteins, such as ankyrin G or βIV spectrin, MAP1A is not present at the Purkinje cell AIS at birth (Y. Liu and S. L. Ackerman, unpublished observations), suggesting that it is necessary for the maintenance, but not the initial specification, of this structure. Consistent with this idea, the Purkinje cell AIS develops normally in *Map1A* mutant mice with morphological defects occurring only after the completion of cerebellar development. The AIS plays an important role in the initiation and modulation of action potentials and, as expected from the unique physiological properties of different neurons, differential localization of multiple ion-channel proteins is observed at the AIS (Bender and Trussell, 2012; Yoshimura and Rasband, 2014). Interestingly, MAP1A is only present at the AIS of Purkinje cells, demonstrating that structural MAPs are also differentially localized at this structure and suggesting that disruption of Purkinje cell AIS by *Map1a* deficiency may contribute to the degeneration of these neurons. Indeed, Purkinje cell-specific ablation of neurofascin, an AIS-localized adhesion molecule, caused disorganization of AIS and progressive degeneration of Purkinje cells (Buttermore et al., 2012).

Last, we show that loss of MAP1A leads to decreased PSD-93 in Purkinje cells. PSD-93 and other MAGUKs play important roles in AMPA and NMDA receptor trafficking along MTs in neuronal processes (Elias et al., 2006; Lau and Zukin, 2007; Sun and Turrigiano, 2011). However, VGlut2 immunostaining did not reveal obvious changes in climbing fiber–Purkinje cell synapses in the *Map1a* mutant cerebellum. Similarly, the parallel fiber–Purkinje cell synapses in the mutant cerebellum appeared normal by TEM (data not shown). Thus it is unlikely that loss of MAP1A directly affects the formation of theses synapses. Rather, it may alter certain aspects of synaptic properties. Indeed, sequence polymorphisms in the mouse *Map1a* gene modify hearing loss caused by the *tubby* mutation, likely through changes in the binding affinity of MAP1A to PSD-95, another member of the MAGUK family (Ikeda et al., 2002). In addition, rare missense mutations in the human *Map1a* gene have been associated with both autism spectrum disorder and schizophrenia (Myers et al., 2011). Further investigations of the *Map1a* mutant mouse models will allow elucidation of the role of these single nucleotide polymorphisms as causal and/or risk factors in human neurological diseases.

References

Ballatore C, Lee VM, Trojanowski JQ (2007) Tau-mediated neurodegeneration in Alzheimer's disease and related disorders. Nat Rev Neurosci 8:663–672. CrossRef Medline

Bender KJ, Trussell LO (2012) The physiology of the axon initial segment. Annu Rev Neurosci 35:249–265. CrossRef Medline

Berezniuk I, Vu HT, Lyons PJ, Sironi JJ, Xiao H, Burd B, Setou M, Angeletti RH, Ikegami K, Fricker LD (2012) Cytosolic carboxypeptidase 1 is involved in processing alpha- and beta-tubulin. J Biol Chem 287:6503–6517. CrossRef Medline

Bonnet C, Boucher D, Lazereg S, Pedrotti B, Islam K, Denoulet P, Larcher JC (2001) Differential binding regulation of microtubule-associated proteins MAP1A, MAP1B, and MAP2 by tubulin polyglutamylation. J Biol Chem 276:12839–12848. CrossRef Medline

Borghesani PR, Alt FW, Bottaro A, Davidson L, Aksoy S, Rathbun GA, Roberts TM, Swat W, Segal RA, Gu Y (2000) Abnormal development of Purkinje cells and lymphocytes in Atm mutant mice. Proc Natl Acad Sci U S A 97:3336–3341. CrossRef Medline

Bouquet C, Soares S, von Boxberg Y, Ravaille-Veron M, Propst F, Nothias F (2004) Microtubule-associated protein 1B controls directionality of growth cone migration and axonal branching in regeneration of adult dorsal root ganglia neurons. J Neurosci 24:7204–7213. CrossRef Medline

Brenman JE, Christopherson KS, Craven SE, McGee AW, Bredt DS (1996) Cloning and characterization of postsynaptic density 93, a nitric oxide synthase interacting protein. J Neurosci 16:7407–7415. Medline

Brenman JE, Topinka JR, Cooper EC, McGee AW, Rosen J, Milroy T, Ralston HJ, Bredt DS (1998) Localization of postsynaptic density-93 to dendritic microtubules and interaction with microtubule-associated protein 1A. J Neurosci 18:8805–8813. Medline

Buttermore ED, Piochon C, Wallace ML, Philpot BD, Hansel C, Bhat MA (2012) Pinceau organization in the cerebellum requires distinct functions of neurofascin in Purkinje and basket neurons during postnatal development. J Neurosci 32:4724–4742. CrossRef Medline

Cambray-Deakin MA, Burgoyne RD (1987) Posttranslational modifications of alpha-tubulin: acetylated and detyrosinated forms in axons of rat cerebellum. J Cell Biol 104:1569–1574. CrossRef Medline

Chien CL, Lu KS, Lin YS, Hsieh CJ, Hirokawa N (2005) The functional cooperation of MAP1A heavy chain and light chain 2 in the binding of microtubules. Exp Cell Res 308:446–458. CrossRef Medline

Conde C, Cáceres A (2009) Microtubule assembly, organization and dynamics in axons and dendrites. Nat Rev Neurosci 10:319–332. CrossRef Medline

Cravchik A, Reddy D, Matus A (1994) Identification of a novel microtubule-binding domain in microtubule-associated protein 1A (MAP1A). J Cell Sci 107:661–672. Medline

Edelmann W, Zervas M, Costello P, Roback L, Fischer I, Hammarback JA, Cowan N, Davies P, Wainer B, Kucherlapati R (1996) Neuronal abnormalities in microtubule-associated protein 1B mutant mice. Proc Natl Acad Sci U S A 93:1270–1275. CrossRef Medline

Elias GM, Funke L, Stein V, Grant SG, Bredt DS, Nicoll RA (2006) Synapse-specific and developmentally regulated targeting of AMPA receptors by a family of MAGUK scaffolding proteins. Neuron 52:307–320. CrossRef Medline

Farley FW, Soriano P, Steffen LS, Dymecki SM (2000) Widespread recombinase expression using FLPeR (flipper) mice. Genesis 28:106–110. CrossRef Medline

Fernandez-Gonzalez A, La Spada AR, Treadaway J, Higdon JC, Harris BS, Sidman RL, Morgan JI, Zuo J (2002) Purkinje cell degeneration (pcd) phenotypes caused by mutations in the axotomy-induced gene, Nna1. Science 295:1904–1906. CrossRef Medline

Goedert M, Jakes R (2005) Mutations causing neurodegenerative tauopathies. Biochim Biophys Acta 1739:240–250. CrossRef Medline

Halpain S, Dehmelt L (2006) The MAP1 family of microtubule-associated proteins. Genome Biol 7:224. CrossRef Medline

Hammarback JA, Obar RA, Hughes SM, Vallee RB (1991) MAP1B is encoded as a polyprotein that is processed to form a complex N-terminal microtubule-binding domain. Neuron 7:129–139. CrossRef Medline

Harada A, Teng J, Takei Y, Oguchi K, Hirokawa N (2002) MAP2 is required for dendrite elongation, PKA anchoring in dendrites, and proper PKA signal transduction. J Cell Biol 158:541–549. CrossRef Medline

Huber G, Matus A (1984a) Differences in the cellular distributions of two

microtubule-associated proteins, MAP1 and MAP2, in rat brain. J Neurosci 4:151–160. Medline

Huber G, Matus A (1984b) Immunocytochemical localization of microtubule-associated protein 1 in rat cerebellum using monoclonal antibodies. J Cell Biol 98:777–781. CrossRef Medline

Iftode F, Clérot JC, Levilliers N, Bré MH (2000) Tubulin polyglycylation: a morphogenetic marker in ciliates. Biol Cell 92:615–628. CrossRef Medline

Ikeda A, Zheng QY, Zuberi AR, Johnson KR, Naggert JK, Nishina PM (2002) Microtubule-associated protein 1A is a modifier of tubby hearing (moth1). Nat Genet 30:401–405. CrossRef Medline

Ikegami K, Heier RL, Taruishi M, Takagi H, Mukai M, Shimma S, Taira S, Hatanaka K, Morone N, Yao I, Campbell PK, Yuasa S, Janke C, Macgregor GR, Setou M (2007) Loss of alpha-tubulin polyglutamylation in ROSA22 mice is associated with abnormal targeting of KIF1A and modulated synaptic function. Proc Natl Acad Sci U S A 104:3213–3218. CrossRef Medline

Janke C, Bulinski JC (2011) Post-translational regulation of the microtubule cytoskeleton: mechanisms and functions. Nat Rev Mol Cell Biol 12:773–786. CrossRef Medline

Janke C, Kneussel M (2010) Tubulin post-translational modifications: encoding functions on the neuronal microtubule cytoskeleton. Trends Neurosci 33:362–372. CrossRef Medline

Janke C, Rogowski K, van Dijk J (2008) Polyglutamylation: a fine-regulator of protein function? 'Protein modifications: beyond the usual suspects' review series. EMBO Rep 9:636–641. CrossRef Medline

Kabeya Y, Mizushima N, Ueno T, Yamamoto A, Kirisako T, Noda T, Kominami E, Ohsumi Y, Yoshimori T (2000) LC3, a mammalian homologue of yeast Apg8p, is localized in autophagosome membranes after processing. EMBO J 19:5720–5728. CrossRef Medline

Kim E, Cho KO, Rothschild A, Sheng M (1996) Heteromultimerization and NMDA receptor-clustering activity of Chapsyn-110, a member of the PSD-95 family of proteins. Neuron 17:103–113. CrossRef Medline

Langkopf A, Hammarback JA, Müller R, Vallee RB, Garner CC (1992) Microtubule-associated proteins 1A and LC2. Two proteins encoded in one messenger RNA. J Biol Chem 267:16561–16566. Medline

Lau CG, Zukin RS (2007) NMDA receptor trafficking in synaptic plasticity and neuropsychiatric disorders. Nat Rev Neurosci 8:413–426. CrossRef Medline

Lee JW, Beebe K, Nangle LA, Jang J, Longo-Guess CM, Cook SA, Davisson MT, Sundberg JP, Schimmel P, Ackerman SL (2006) Editing-defective tRNA synthetase causes protein misfolding and neurodegeneration. Nature 443:50–55. CrossRef Medline

Lei P, Ayton S, Finkelstein DI, Spoerri L, Ciccotosto GD, Wright DK, Wong BX, Adlard PA, Cherny RA, Lam LQ, Roberts BR, Volitakis I, Egan GF, McLean CA, Cappai R, Duce JA, Bush AI (2012) Tau deficiency induces parkinsonism with dementia by impairing APP-mediated iron export. Nat Med 18:291–295. CrossRef Medline

Liu Y, Zaun HC, Orlowski J, Ackerman SL (2013) CHP1-mediated NHE1 biosynthetic maturation is required for Purkinje cell axon homeostasis. J Neurosci 33:12656–12669. CrossRef Medline

Mann SS, Hammarback JA (1994) Molecular characterization of light chain 3. A microtubule binding subunit of MAP1A and MAP1B. J Biol Chem 269:11492–11497. Medline

McGee AW, Topinka JR, Hashimoto K, Petralia RS, Kakizawa S, Kauer FW, Aguilera-Moreno A, Wenthold RJ, Kano M, Bredt DS, Kauer F (2001) PSD-93 knock-out mice reveal that neuronal MAGUKs are not required for development or function of parallel fiber synapses in cerebellum. J Neurosci 21:3085–3091. Medline

Meixner A, Haverkamp S, Wässle H, Führer S, Thalhammer J, Kropf N, Bittner RE, Lassmann H, Wiche G, Propst F (2000) MAP1B is required for axon guidance and is involved in the development of the central and peripheral nervous system. J Cell Biol 151:1169–1178. CrossRef Medline

Mullen RJ, Eicher EM, Sidman RL (1976) Purkinje cell degeneration, a new neurological mutation in the mouse. Proc Natl Acad Sci U S A 73:208–212. CrossRef Medline

Myers RA, Casals F, Gauthier J, Hamdan FF, Keebler J, Boyko AR, Bustamante CD, Piton AM, Spiegelman D, Henrion E, Zilversmit M, Hussin J, Quinlan J, Yang Y, Lafrenière RG, Griffing AR, Stone EA, Rouleau GA, Awadalla P (2011) A population genetic approach to mapping neurological disorder genes using deep resequencing. PLoS Genet 7:e1001318. CrossRef Medline

Palay SL, Sotelo C, Peters A, Orkand PM (1968) The axon hillock and the initial segment. J Cell Biol 38:193–201. CrossRef Medline

Paturle-Lafanechère L, Manier M, Trigault N, Pirollet F, Mazarguil H, Job D (1994) Accumulation of delta 2-tubulin, a major tubulin variant that cannot be tyrosinated, in neuronal tissues and in stable microtubule assemblies. J Cell Sci 107:1529–1543. Medline

Reese ML, Dakoji S, Bredt DS, Dötsch V (2007) The guanylate kinase domain of the MAGUK PSD-95 binds dynamically to a conserved motif in MAP1a. Nat Struct Mol Biol 14:155–163. CrossRef Medline

Riederer B, Matus A (1985) Differential expression of distinct microtubule-associated proteins during brain development. Proc Natl Acad Sci U S A 82:6006–6009. CrossRef Medline

Roche KW, Ly CD, Petralia RS, Wang YX, McGee AW, Bredt DS, Wenthold RJ (1999) Postsynaptic density-93 interacts with the δ2 glutamate receptor subunit at parallel fiber synapses. J Neurosci 19:3926–3934. Medline

Rogowski K, van Dijk J, Magiera MM, Bosc C, Deloulme JC, Bosson A, Peris L, Gold ND, Lacroix B, Bosch Grau M, Bec N, Larroque C, Desagher S, Holzer M, Andrieux A, Moutin MJ, Janke C (2010) A family of protein-deglutamylating enzymes associated with neurodegeneration. Cell 143:564–578. CrossRef Medline

Schoenfeld TA, McKerracher L, Obar R, Vallee RB (1989) MAP 1A and MAP 1B are structurally related microtubule associated proteins with distinct developmental patterns in the CNS. J Neurosci 9:1712–1730. Medline

Shiomura Y, Hirokawa N (1987a) The molecular structure of microtubule-associated protein 1A (MAP1A) *in vivo* and *in vitro*. An immunoelectron microscopy and quick-freeze, deep-etch study. J Neurosci 7:1461–1469. Medline

Shiomura Y, Hirokawa N (1987b) Colocalization of microtubule-associated protein 1A and microtubule-associated protein 2 on neuronal microtubules in situ revealed with double-label immunoelectron microscopy. J Cell Biol 104:1575–1578. CrossRef Medline

Sun Q, Turrigiano GG (2011) PSD-95 and PSD-93 play critical but distinct roles in synaptic scaling up and down. J Neurosci 31:6800–6808. CrossRef Medline

Szebenyi G, Bollati F, Bisbal M, Sheridan S, Faas L, Wray R, Haferkamp S, Nguyen S, Caceres A, Brady ST (2005) Activity-driven dendritic remodeling requires microtubule-associated protein 1A. Curr Biol 15:1820–1826. CrossRef Medline

Teng J, Takei Y, Harada A, Nakata T, Chen J, Hirokawa N (2001) Synergistic effects of MAP2 and MAP1B knockout in neuronal migration, dendritic outgrowth, and microtubule organization. J Cell Biol 155:65–76. CrossRef Medline

Twyman RM, Jones EA (1997) Sequences in the proximal 5′ flanking region of the rat neuron-specific enolase (NSE) gene are sufficient for cell type-specific reporter gene expression. J Mol Neurosci 8:63–73. CrossRef Medline

Vaillant AR, Müller R, Langkopf A, Brown DL (1998) Characterization of the microtubule-binding domain of microtubule-associated protein 1A and its effects on microtubule dynamics. J Biol Chem 273:13973–13981. CrossRef Medline

Vallee RB, Davis SE (1983) Low molecular weight microtubule-associated proteins are light chains of microtubule-associated protein 1 (MAP 1). Proc Natl Acad Sci U S A 80:1342–1346. CrossRef Medline

Wloga D, Gaertig J (2010) Post-translational modifications of microtubules. J Cell Sci 123:3447–3455. CrossRef Medline

Yoshimura T, Rasband MN (2014) Axon initial segments: diverse and dynamic neuronal compartments. Curr Opin Neurobiol 27:96–102. CrossRef Medline